



HAL
open science

Comparison between x-ray diffraction and quantitative surface calorimetry based on infrared thermography to evaluate strain-induced crystallinity in natural rubber

Jean-Benoit Le Cam, P. -A. Albouy, Sylvain Charles

► **To cite this version:**

Jean-Benoit Le Cam, P. -A. Albouy, Sylvain Charles. Comparison between x-ray diffraction and quantitative surface calorimetry based on infrared thermography to evaluate strain-induced crystallinity in natural rubber. *Review of Scientific Instruments*, 2020, 91 (4), 10.1063/1.5141851 . hal-02562286v2

HAL Id: hal-02562286

<https://univ-rennes.hal.science/hal-02562286v2>

Submitted on 7 May 2020 (v2), last revised 15 May 2020 (v3)

HAL is a multi-disciplinary open access archive for the deposit and dissemination of scientific research documents, whether they are published or not. The documents may come from teaching and research institutions in France or abroad, or from public or private research centers.

L'archive ouverte pluridisciplinaire **HAL**, est destinée au dépôt et à la diffusion de documents scientifiques de niveau recherche, publiés ou non, émanant des établissements d'enseignement et de recherche français ou étrangers, des laboratoires publics ou privés.

Comparison between x-ray diffraction and quantitative surface calorimetry based on infrared thermography to evaluate strain-induced crystallinity in natural rubber

J.-B. Le Cam,^{1,a)} P.-A. Albouy,² and S. Charlès¹

AFFILIATIONS

¹Univ. Rennes, CNRS, IPR (Institut de Physique de Rennes), UMR 6251, F-35000 Rennes, France

²Laboratoire de Physique des Solides, CNRS, Université Paris-Sud, Université Paris-Saclay, 91405 Orsay, France

^{a)} Author to whom correspondence should be addressed: jean-benoit.lecam@univ-rennes1.fr

ABSTRACT

The crystallinity of stretched crystallizable rubbers is classically evaluated using x-ray diffraction (XRD). As crystallization is a strongly exothermal phenomenon, quantitative surface calorimetry from infrared thermography offers an interesting alternative to XRD for determining the crystallinity. In this paper, the two measurement techniques have been used for evaluating the strain-induced crystallinity of the same unfilled natural rubber. This study provides the first comparison between the two techniques. The results obtained highlight the very satisfactory agreement between the two measurements, which opens a simple way for evaluating the strain-induced crystallinity from temperature measurements.

I. INTRODUCTION

Since the pioneering work by Katz in 1925,¹ who obtained the first x-ray diffraction (XRD) pattern of a stretched natural rubber (NR), the strain-induced crystallization (SIC) of rubber is classically investigated using XRD. XRD provides not only the crystallinity but also the information of paramount importance on the crystalline phase structure,²⁻⁵ chain orientation,⁶ and kinetics of crystallization,^{7,8} non-exhaustively.

Concerning the crystallinity measurement, Göritz and co-workers showed in the 1970s that strain-induced crystallinity could be quantified accurately with an alternative technique, based on “stretch calorimetry.”⁹ Indeed, crystallization is strongly exothermal and the corresponding crystallinity can therefore be evaluated from the part of the total heat source¹⁰ that is produced by SIC only. This technique offered a simpler way than XRD to evaluate the crystallinity. Despite this, calorimetry under stretching was no longer used to measure crystallinity. A possible reason could be that the crystallinity obtained was averaged over all the specimen. Therefore, it is not possible to address heterogeneous crystallinity fields

typically at the crack tip of a notched specimen.^{11,12} With the advent of non-contact measurement techniques, it has been demonstrated that the calorimetric response could be directly obtained at the surface of a thin specimen as soon as the heat diffusion by conduction and convection is characterized and that no temperature gradient occurs in the specimen thickness.¹³ This technique has been successfully employed for characterizing the calorimetric signature of phenomena involved in the rubber deformation under homogeneous strain states^{14,15} and at the crack tip where the mechanical and calorimetric field are strongly heterogeneous.^{16,17} Furthermore, such a technique enables us to make energy balance and to identify the intrinsic dissipation.¹⁸⁻²⁰

Recently, Le Cam has proposed to couple the work by Göritz and Müller and the IR thermography-based surface calorimetry approach to evaluate the strain-induced crystallinity.²¹ By this way, Le Cam measured the crystallinity induced in an unfilled natural rubber submitted to a mechanical tensile cycle. Even though the crystallinity found seems to be in good agreement with the literature, no validation was done by comparing the result obtained and that obtained with XRD for the same material. This is the aim of

this study. In the first part of the paper, the framework for evaluating the strain-induced crystallinity from the two techniques is presented. The second part of the paper details the experiments carried out and compares the two measurements performed. Concluding remarks close the paper.

II. XRD TECHNIQUE

Crystallinity indices reported here are derived from an analysis of angular scans centered on the amorphous halo, as detailed in Ref. 22. This method combines simplicity and direct access to the Herman orientation parameter for the amorphous phase. Further parameters provided by XRD include the crystallite dimensions and their orientation with respect to the draw axis (see the references cited in the Introduction). One main limitation for the use of XRD is that it requires the installation of a testing machine on a laboratory diffraction bench, which is out of the reach of many laboratories. In the present case, the testing machine is installed on a rotating anode generator operated at medium power (copper anode, 40 kV, 40 mA, focus size of $0.2 \times 0.2 \text{ mm}^2$). The CuK_α radiation is selected with a doubly curved graphite monochromator with a focalization distance of 24 cm. The sample is located at the focalization point, which ensures optimized diffracted intensity. The setup can be equipped with an indirect illumination CCD camera or a hybrid pixel detector. This last x-ray camera combines high efficiency and the absence of noise, and acquisition times as low as 0.2 s per frame with good counting statistics are possible.²³ The drawing speed can be selected between 1 mm/min and 800 mm/min. However, the necessity of collecting a sufficient number of frames (acquisition time: 0.2 s) during the stretching phase limited the maximal drawing speed to 200 mm/min. The incident beam diameter is $\sim 1 \text{ mm}$ in that case, which precludes any detailed analysis of heterogeneous zones if any. Much smaller beam spots can be reached with special optics at the price of intensity loss, and systematic mapping becomes highly time consuming.

III. QUANTITATIVE SURFACE CALORIMETRY FROM IR THERMOGRAPHY (IRT-QSC)

SIC is a strongly exothermal phenomenon, which explains why surface calorimetry is a relevant alternative to determine the crystallinity. Crystallinity can be evaluated from the part of the total heat source that is produced by SIC only, which gives access to the corresponding crystallization temperature T_{cryst} . The crystallinity χ can then be deduced from T_{cryst} by considering that the crystallization energy of the natural rubber can be approximated by the enthalpy of fusion ΔH_{cryst} (in J/dm^3),^{21,24}

$$\chi(t) = \frac{\rho C T_{cryst}(t)}{\Delta H_{cryst}}. \quad (1)$$

ρ and C are, respectively, the material's density (in kg/dm^3) and the heat capacity [in $\text{J}/(\text{kg K})$]. The material's density and heat capacity are assumed to be independent of strain and temperature.

Determining strain-induced crystallinity from infrared (IR) thermography has several advantages:

- the crystallinity field is measured instantaneously, which is of paramount importance in the case of a heterogeneous crystallinity field

- IR thermography provides high resolution thermal measurements (temporal, spatial, and on the value of the crystallinity itself through the thermal resolution of 20 mK in the temperature range of the present experiment),
- the measurement can be performed in any lab equipped with a conventional testing machine, and
- the heat source produced by SIC can be directly linked with constitutive equations through the thermomechanical couplings. Therefore, this technique is all the more interesting that it enables us to validate and to improve thermomechanical SIC models.

Nevertheless, this technique does not provide information on the crystalline phase structure and chain orientation. In Sec. IV, the thermomechanical framework used to determine the heat source and the crystallization temperature due to SIC is presented.

IV. HEAT SOURCE RECONSTRUCTION

Most of the mechanical tests are conducted under non-adiabatic conditions. The temperature measured is therefore affected by heat diffusion within the specimen and with the specimen outside. Therefore, changes in temperature are not only due to the material deformation itself, and the heat diffusion equation is used to determine the corresponding heat source from temperature measurement. This quantity is intrinsic to the material deformation and can be directly compared with constitutive model predictions. Thus, any temperature measurement technique can be used as a calorimeter, an IR camera in this study, as soon as the heat diffusion by conduction and convection is characterized. In the thermodynamic framework applied, any thermodynamical system out of equilibrium is considered as the sum of several homogeneous subsystems at equilibrium. The deformation is considered as a quasi-static thermodynamic process. The equilibrium state of each volume material element is defined by n state variables: the absolute temperature T , the deformation gradient tensor \mathbf{F} , and $m (=n - 2)$ internal tensorial variables ξ_α . The local form of the heat diffusion equation is written as follows in the Lagrangian configuration

$$\rho C \dot{T} - \text{Div}(\kappa_0 \text{Grad } T) = R + \underbrace{\mathcal{D}_{int} + T \frac{\partial \mathbf{P}}{\partial T} : \dot{\mathbf{F}} + T \sum_{\beta=1}^m \frac{\partial A_\beta}{\partial T} : \dot{\xi}_\beta}_S, \quad (2)$$

where κ_0 is a positive semi-definite tensor characterizing the thermal conductivity of the material. R stands for the external heat source due to radiation. S denotes the overall heat source induced by the deformation process. The term \mathcal{D}_{int} corresponds to the intrinsic dissipation. The term $T \frac{\partial \mathbf{P}}{\partial T} : \dot{\mathbf{F}}$ is the heat source due to couplings between temperature and strain, where \mathbf{P} is the nominal stress tensor. The term $T \frac{\partial A_\beta}{\partial T} : \dot{\xi}_\beta$ corresponds to the other thermomechanical couplings (for instance, related to phase change in the material). Let us denote θ as the temperature variation with respect to the equilibrium temperature T^{ref} in the reference state, corresponding to the undeformed state (T^{ref} is constant and equal to the ambient temperature). In the case where changes in ambient temperature occur, T^{ref} has to be corrected accordingly with the measurement of ambient temperature variations. Moreover, in the case where the heat conduction in the specimen plane is neglected, the tri-dimensional

formulation of the heat diffusion equation can be simplified and written in the case of the homogeneous heat source field. After some calculations that are not detailed here, the heat diffusion equation can be rewritten in the case of the homogeneous heat source field¹³

$$\rho C \left(\dot{\theta} + \frac{\theta}{\tau} \right) = S, \quad (3)$$

where τ is a parameter characterizing the heat exchanges between the specimen and its surroundings.²⁵ It can be easily identified from a natural return to room temperature after a heating (or a cooling) for each testing configuration (machine used, environment, etc.). For instance, in the case where the material is beforehand heated,

the exponential formulation of the temperature variation is used to determine parameter τ , $\theta = \theta_0 e^{-\frac{(t-t_0)}{\tau}}$. In the case of large deformations, τ depends on the stretch. Either τ is determined at different increasing stretches (further details are provided in Ref. 14), or the value of τ is corrected according to its dependency on the stretch in the case of incompressible materials. In the former case, the determination of τ during the natural return to ambient temperature for stretches higher than that at which crystallization starts is affected by the fact that additional heat is produced (absorbed) due to crystallization (melting) during the material cooling (heating). This is the reason why in the present study $\tau(\lambda)$ has been determined from its value in the undeformed state (denoted τ_0) and the link between the

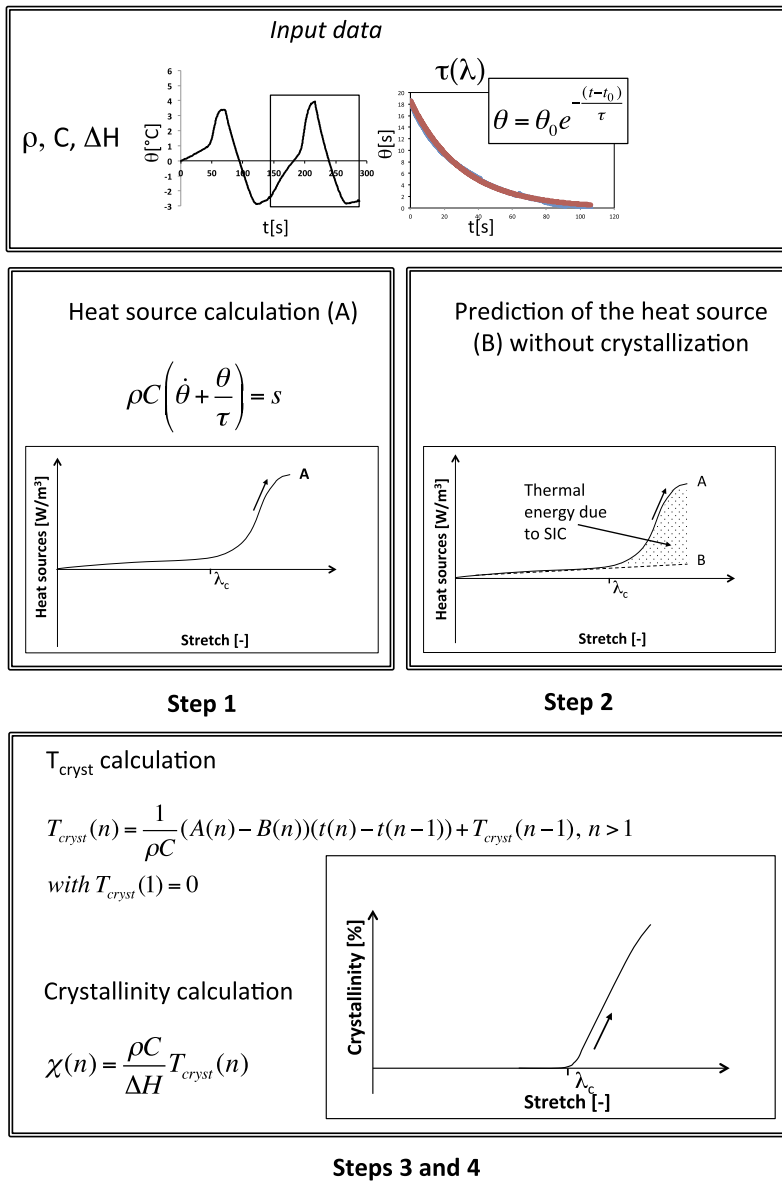


FIG. 1. Methodology for determining crystallinity from temperature variation measurement.

thickness and the stretch. This link depends on the biaxiality ratio B , define as the ratio between the logarithm of λ_2 and the logarithm of λ_1 . λ_1 and λ_2 are the maximum and minimum principal stretches in the specimen plane, respectively. By assuming the material to be incompressible, τ writes

$$\tau = \tau(\lambda, B) = \tau_0 \lambda^{-B-1}. \quad (4)$$

In the present case of the uniaxial tension, B is equal to -0.5 and τ is written finally as

$$\tau(\lambda) = \frac{\tau_0}{\sqrt{\lambda}}. \quad (5)$$

A. Determination of the crystallinity

Figure 1 illustrates the methodology proposed. It requires the temperature variation θ , the parameter τ , and the thermophysical parameters ρ , C , and ΔH as input data, and is composed of four steps:

- **Step 1:** the heat source is calculated by applying Eq. (3). The diagram illustrates the typical increase in the heat source produced in unfilled NR once crystallization starts.^{9,14} Here, λ_c stands for the stretch at which SIC starts.
- **Step 2:** the thermal energy due to SIC is deduced from the area located between the heat source measured (curve A) and the part of the heat source that would be due to the elastic coupling only (curve B). The latter is predicted by using a polynomial, whose parameters are identified by fitting the heat source measured before SIC starts ($\lambda < \lambda_c$), $C_1(\lambda - \lambda^{-2}) + C_2(\lambda - \lambda^{-2})^2 + C_3(\lambda - \lambda^{-2})^3$. It should be noted that a first or second order polynomial also provides satisfactory results.
- **Step 3:** T_{cryst} is computed from the heat source due to SIC, i.e., the area between curves A and B. See, for instance, the not centered numerical scheme given in Fig. 1.
- **Step 4:** the crystallinity is calculated by applying Eq. (1).

This method is very simple and does not require measuring the nominal stress variations nor characterizing possible non-entropic effects²⁶ because they are included in the calorimetric response.

V. EXPERIMENTS

The material considered here is an unfilled natural rubber of grade SMR 5L vulcanized by sulfur ($1.5phr$) in the presence of conventional activators and antioxidant agents. The average molecular weight between cross-links is 6330 g mol^{-1} (86 isoprene units) based on mechanical measurements. For the calculations, the density, specific heat, and fusion enthalpy values were chosen equal to 0.936 kg/dm^3 , 1768 J/(kg K) , and $62 \cdot 10^3 \text{ J/dm}^3$, respectively. The mechanical loading is applied symmetrically at a stretch equal to 7.2 and two different loading rates of 100 mm/min and 200 mm/min . The averaged specimen dimensions were 19.3 mm in height, 7.2 mm in width, and 1.4 mm in thickness. The experimental setup used for the XRD technique is depicted in Fig. 2.

The experimental setup used for the temperature measurement is presented in Fig. 3. Tests were conducted with a home-made biaxial testing machine. Four independent electrical actuators enable us to stretch symmetrically the specimens in two

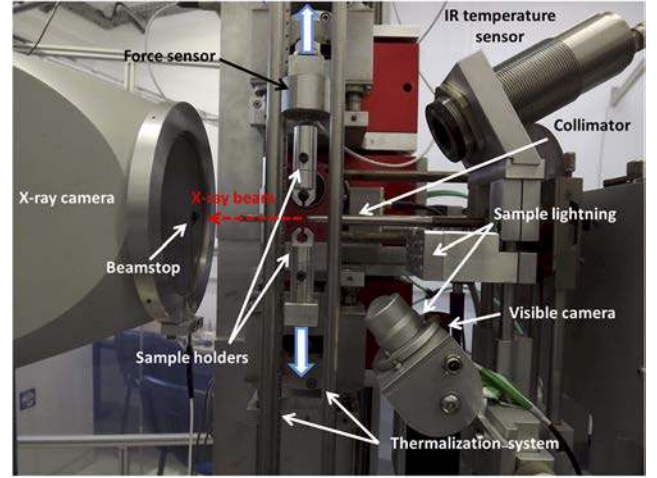


FIG. 2. Experimental setup for the XRD technique.

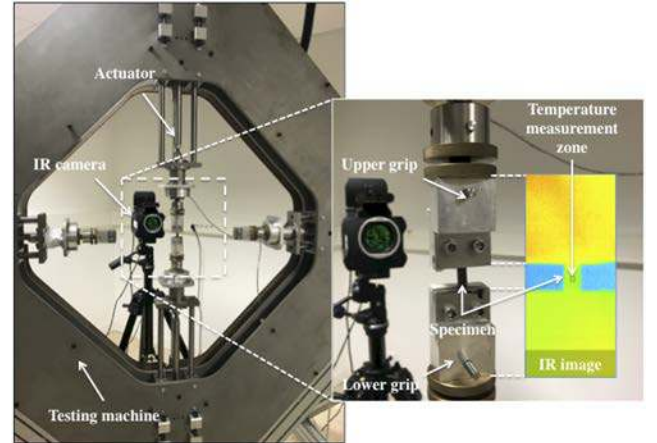


FIG. 3. Experimental setup for the temperature measurement.

perpendicular directions. Actuators are driven by means of a home-made LabVIEW program. The cell load capacity is 1094 N . In the present case, the testing machine is used to stretch symmetrically the specimen in one direction only. Therefore, the zone where the thermal measurement is performed remains in the same place, which enables us to obtain the temperature variation by subtracting the current measurement zone to the initial one, without any motion compensation technique.²⁷ In order to reduce the external radiation, the grips were covered with a black body leaf (see the IR image in Fig. 3).

VI. RESULTS

Figure 4 presents the mechanical responses obtained in terms of the nominal stress, defined as the force per unit surface, in relation to the stretch for the two loading rates during the two types of

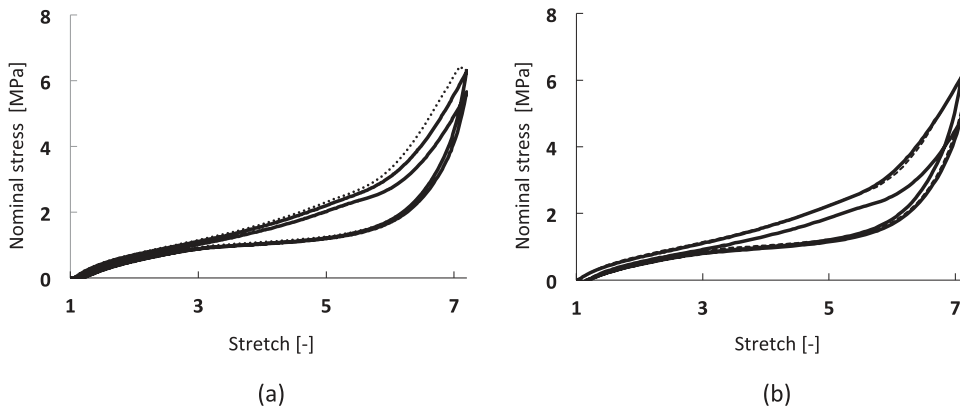


FIG. 4. Mechanical response obtained: XRD experiments in dotted line and IRT experiments in continuous line: (a) 100 mm/min and (b) 200 mm/min.

measurement. The continuous and dotted lines are the mechanical responses obtained with the tensile machine used for IR thermography and XRD measurements, respectively.

The thermal response is shown with red curves in Fig. 5. Figure 5 shows the typical response of a crystallizing rubber, i.e., a strong temperature increase occurs once the crystallization stretch onset is exceeded. It should be noted that the temperature increases at the end of the unloading. This is due to non-adiabatic effects that are all the more significant that the loading rate is low. Further explanations on non-adiabatic effects on the temperature variation are provided in Ref. 28 (pp. 2721–2722).

The corresponding adiabatic temperature variations (black curves in Fig. 5) are deduced from the heat source. The fact that

$\tau(\lambda)$ enables us to retrieve a temperature equal to zero at the end of each cycle validates the characterization of the non-adiabatic effects, i.e., the value of τ , as the material does not produce heat at each mechanical cycle.

Figure 6 depicts the heat source in relation to the stretch (curve A), obtained from Eq. (3) (step 1). During loading, the heat source is positive and increases with the stretch. Once SIC starts, a strong increase in the heat produced is observed. The polynomial form in step 2 is used to predict the heat source due to elastic couplings and to determine the area between the two curves, i.e., the thermal energy, due to SIC only. Then, the crystallization temperature is obtained from the primitive calculation of the heat source²⁹ due to SIC.

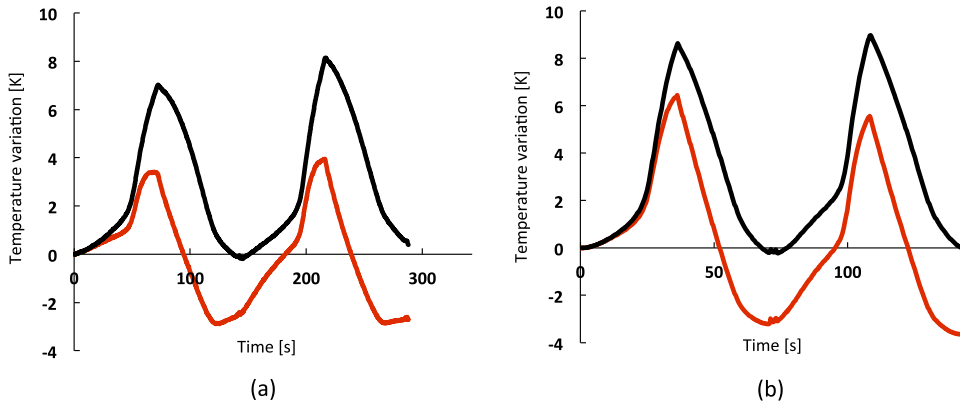


FIG. 5. Temperature variation measured (in red) and the corresponding adiabatic one (in black) during the first two cycles: (a) 100 mm/min and (b) 200 mm/min.

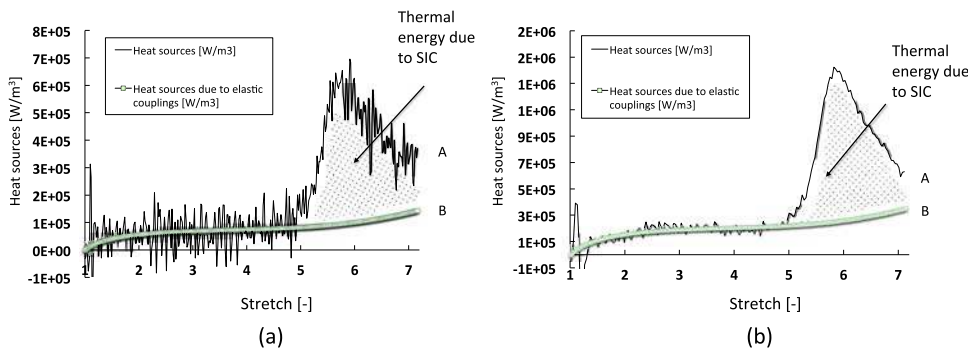


FIG. 6. Heat source, strain power density, and heat source due to elastic couplings during loading No. 2: (a) 100 mm/min and (b) 200 mm/min.

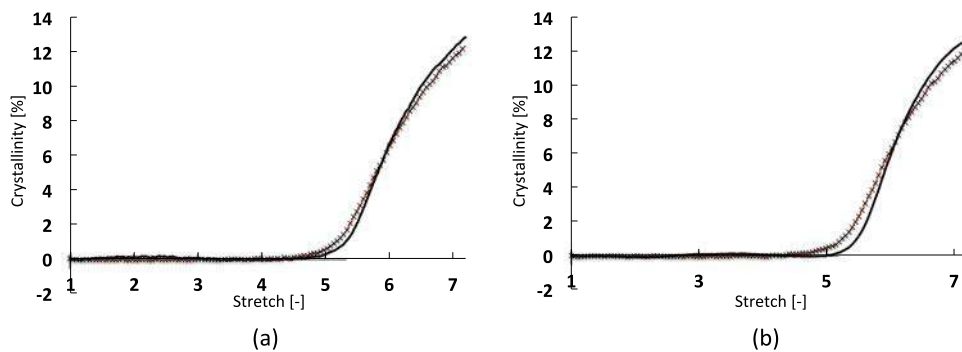


FIG. 7. Crystallinity in % during loading No. 2 (—) surface calorimetry (x) XRD: (a) 100 mm/min and (b) 200 mm/min.

The integration constant is determined considering that T_{cryst} before crystallization starts is equal to zero. It should be noted that without any crystallization, i.e., below the strain at which crystallization starts during the loading, T_{cryst} is equal to zero, i.e., no temperature variation is due to SIC. Indeed, for this unfilled NR formulation, the XRD measurements have shown that the crystallinity returns to zero at the end of each cycle. The crystallinity is calculated by using the fusion enthalpy. The crystallinity obtained for the two loading rates applied corresponds to the continuous lines in Fig. 7. The XRD measurement, which was performed during the first loading, corresponds to lines with cross symbols. This comparison clearly shows the relevancy of evaluating strain-induced crystallization from IR thermography measurements.

VII. CONCLUSION

In this study, the crystallinity of an unfilled natural rubber has been evaluated by two different techniques: the IR thermography based quantitative surface calorimetry (IRT-QSC) and the x-ray diffraction (XRD) techniques. The results obtained highlight a very satisfactory agreement between the two measurements, which validates the IR-QSC technique proposed in Le Cam (2018) to measure the strain-induced crystallinity. Further investigations are currently carried out by coupling the two techniques for a better characterization of the thermo-physical properties and their evolution with the stretch. It is important to note that x-ray diffraction is also complementary of temperature measurements at low drawing velocity where calorimetric effects become hardly detectable.

AUTHOR'S CONTRIBUTIONS

J.-B.L.C., P.-A.A., and S.C. contributed equally to this work.

ACKNOWLEDGMENTS

The data that support the findings of this study are available from the corresponding author upon reasonable request.

REFERENCES

¹J. R. Katz, "Röntgenspektrographische Untersuchungen am gedehnten Kautschuk und ihre mögliche Bedeutung für das Problem der Dehnungseigenschaften dieser Substanz," *Naturwiss.* **13**, 410 (1925).
²C. Bunn, *Proc. R. Soc. London, Ser. A* **180**, 1 (1942).

³Y. Takahashi and T. Kumano, "Crystal structure of natural rubber," *Macromolecules* **37**, 4860 (2004).
⁴A. Immirzi, C. Tedesco, G. Monaco, and A. E. Tonelli, "Crystal structure and melting entropy of natural rubber," *Macromolecules* **38**, 1223 (2005).
⁵G. Rajkumar, J. M. Squire, and S. Arnott, "A new structure for crystalline natural rubber," *Macromolecules* **39**, 7004 (2006).
⁶S. Toki, I. Sics, B. S. Hsiao, S. Murakami, M. Tosaka, S. Poompradub, S. Kohjiya, and Y. Ikeda, "Structural developments in synthetic rubbers during uniaxial deformation by in situ synchrotron X-ray diffraction," *J. Polym. Sci. B: Polym. Phys.* **42**, 956 (2004).
⁷S. Toki, T. Fujimaki, and M. Okuyama, "Strain-induced crystallization of natural rubber as detected real-time by wide-angle x-ray diffraction technique," *Polymer* **41**, 5423–5429 (2000).
⁸S. Trabelsi, P.-A. Albouy, and J. Rault, "Effective local deformation in stretched filled rubber," *Macromolecules* **36**, 9093–9099 (2003).
⁹D. Göritz and F. H. Müller, "Die kalorimetrische erfassung der dehnungskristallisation polymerer," *Kolloid-Z. Z. Polym.* **241**, 1075–1079 (1970).
¹⁰The term "heat source" is used in this paper to mean the heat power density in W/m^3 , which is produced or absorbed by the material.
¹¹S. Trabelsi, P.-A. Albouy, and J. Rault, "Stress-induced crystallization around a crack tip in natural rubber," *Macromolecules* **35**, 10054–10061 (2002).
¹²P. Rublon, B. Huneau, E. Verron, N. Saintier, S. Beurrot, A. Leygue, C. Mocuta, D. Thiaudière, and D. Berghezan, "Multiaxial deformation and strain-induced crystallization around a fatigue crack in natural rubber," *Eng. Fract. Mech.* **123**, 59–69 (2014).
¹³A. Chrysochoos, "Analyse du comportement des matériaux par thermographie infra rouge," *Colloq. Photomécanique* **95**, 201–211 (1995).
¹⁴J. R. Samaca Martinez, J.-B. Le Cam, X. Balandraud, E. Toussaint, and J. Caillard, "Mechanisms of deformation in crystallizable natural rubber. Part 2: Quantitative calorimetric analysis," *Polymer* **54**, 2727–2736 (2013).
¹⁵J.-B. Le Cam, J. R. Samaca Martinez, X. Balandraud, E. Toussaint, and J. Caillard, "Thermomechanical analysis of the singular behavior of rubber: Entropic elasticity, reinforcement by fillers strain-induced crystallization and the Mullins effect," *Exp. Mech.* **55**, 771–782 (2015).
¹⁶J. R. Samaca Martinez, X. Balandraud, E. Toussaint, and J.-B. Le Cam, and D. Berghezan, "Thermomechanical analysis of the crack tip zone in stretched crystallizable natural rubber by using infrared thermography and digital image correlation," *Polymer* **55**, 6345–6353 (2014).
¹⁷J. R. Samaca Martinez, E. Toussaint, X. Balandraud, J.-B. Le Cam, and D. Berghezan, "Heat and strain measurements at the crack tip of filled rubber under cyclic loadings using full-field techniques," *Mech. Mater.* **81**, 62–71 (2015).
¹⁸J.-B. Le Cam, "Energy storage due to strain-induced crystallization in natural rubber: The physical origin of the mechanical hysteresis," *Polymer* **127**, 166–173 (2017).
¹⁹A. Lachhab, E. Robin, J.-B. Le Cam, F. Mortier, Y. Tirel, and F. Canevet, "Energy stored during deformation of crystallizing TPU foams," *Strain* **54**, e12271 (2018).
²⁰M. T. Loukil, G. Corvec, E. Robin, M. Miroir, J.-B. Le Cam, and P. Garnier, "Stored energy accompanying cyclic deformation of filled rubber," *Eur. Polym. J.* **98**, 448–455 (2018).

- ²¹J.-B. Le Cam, "Strain-induced crystallization in rubber: A new measurement technique," *Strain* **54**, e12256 (2018).
- ²²P.-A. Albouy, A. Vieyres, R. Pérez-Aparicio, O. Sanséau, and P. Sotta, "The impact of strain-induced crystallization on strain during mechanical cycling of cross-linked natural rubber," *Polymer* **55**, 4022–4031 (2014).
- ²³P.-A. Albouy and P. Sotta, "Draw ratio at the onset of strain-induced crystallization in cross-linked natural rubber," *Macromolecules* **53**, 992–1000 (2020).
- ²⁴T. Spratte, J. Plagge, M. Wunde, and M. Klüppel, "Investigation of strain-induced crystallization of carbon black and silica filled natural rubber composites based on mechanical and temperature measurements," *Polymer* **115**, 12–20 (2017).
- ²⁵In this case, only a one-point temperature measurement is required, meaning that the crystallinity can be evaluated with a pyrometer.
- ²⁶L. R. G. Treloar, "The elasticity and related properties of rubbers," *Rep. Prog. Phys.* **36**, 755 (1973).
- ²⁷E. Toussaint, X. Balandraud, J.-B. Le Cam, and M. Grédiac, "Combining displacement, strain, temperature and heat source field to investigate the thermo-mechanical response of an elastomeric specimen subjected to large deformations," *Polym. Test.* **31**, 916–925 (2012).
- ²⁸J. R. Samaca Martinez, J.-B. Le Cam, X. Balandraud, E. Toussaint, and J. Cailhard, "Mechanisms of deformation in crystallizable natural rubber. Part 1: Thermal characterization," *Polymer* **54**, 2717–2726 (2013).
- ²⁹Here, the heat source is expressed in $^{\circ}/s$, i.e. $\frac{S}{\rho C}$.